Inorganica Chimica Acta 602 (2026) 123348

Contents lists available at ScienceDirect

Inorganica Chimica Acta

journal homepage: www.elsevier.com/locate/ica

Cyclopentadienyl vs indenyl control of thermal/photoactivated CO release in cationic molybdenum(II) dicarbonyl-ethylenediamine complexes

Sofia M. Bruno [a], Isabel B. Calhau [a], Tiago M. Dias [a], Adriana Santos [a], Luís Cunha-Silva [b,c], Mariela M. Nolasco [a], Isabel S. Gonçalves [a], Martyn Pillinger [a,*]

[a] CICECO - Aveiro Institute of Materials, Department of Chemistry, University of Aveiro, Campus Universitário de Santiago, 3810-193 Aveiro, Portugal
[b] LAQV / REQUIMTE & Department of Chemistry and Biochemistry, Faculty of Sciences, University of Porto, 4169-007 Porto, Portugal
[c] LNEG, Nacional Laboratory of Energy and Geology, I.P., Campus do Lumiar, 1649-038 Lisboa, Portugal

ARTICLE INFO

Keywords:
Half-sandwich complexes
Molybdenum
Crystal structure
Indenyl
Cyclopentadienyl
CO-releasing molecules
photoCORMs

ABSTRACT

Molybdenum half-sandwich carbonyl complexes continue to attract attention as potential anticancer agents and prodrugs for therapeutic use of carbon monoxide. Building on the known bioactivity and hydrolytic stability of cyclopentadienyl-based Mo fragments, we report the synthesis, structural characterization, and solution behavior of two cationic half-sandwich complexes, $[(\eta^5\text{-Cp})Mo(CO)_2(en)][BF_4]$ (**3**) and $[(\eta^5\text{-Ind})Mo(CO)_2(en)][BF_4]$ (**4**) (Cp = cyclopentadienyl, Ind = indenyl, en = ethylenediamine). Complex **3** is described here for the first time, while **4** was structurally characterized by single-crystal X-ray diffraction, revealing a distorted square-pyramidal geometry with cis-CO ligands and a chelating en ligand positioned beneath the indenyl ring. Both compounds are air-stable in the solid state and exhibit enhanced solubility in polar media due to their ionic nature. UV–vis stability studies under simulated physiological conditions (PBS, pH 7.4, 37 °C) show gradual decomposition of both complexes, accelerated by visible-light irradiation and/or the presence of air. CO-release behavior was quantified using the myoglobin assay: the allyl precursors $[(\eta^5\text{-Cp}')Mo(\eta^3\text{-}C_3H_5)(CO)_2]$ were inert, whereas complexes **3** and **4** released CO slowly, with **4** exhibiting significantly faster thermal CO liberation ($t_{1/2} \approx 129$ min; 0.74 equiv. CO after 6 h). Complex **3** showed minimal thermal CO release but underwent enhanced and sustained photodecarbonylation under visible-light irradiation, enabling controlled CO delivery. These results identify **3** and **4** as rare examples of Mo-based CO-releasing molecules capable of slow, tunable CO release under biologically relevant conditions, with **3** displaying light-responsive behavior and **4** functioning as a spontaneous thermal CO donor.

1. Introduction

In the field of bioorganometallic chemistry, molybdenum complexes have been increasingly studied, mainly in the context of anticancer chemotherapy [1–31]. The trigger for this research was the discovery in the late 1970s that molybdenocene dichloride, $(\eta^5\text{-Cp})_2MoCl_2$ (Cp = C_5H_5) was active in vivo against a variety of tumors [3]. Unlike titanocene dichloride, which advanced as far as phase II clinical trials in the 1990s, the Cp_2Mo^{2+} fragment has good hydrolytic stability at physiological pH [10], which encouraged efforts to improve the anticancer activity by replacing the chloride ligands and/or functionalizing the cyclopentadienyl ligands [4–9]. Promising cytotoxic properties were also reported for monocyclopentadienyl and indenyl (η^5-Cp') compounds of the type $[(\eta^5\text{-Cp}')Mo(CO)_2(^{NN}L)][BF_4]$, where ^{NN}L is a *N,N*-chelating ligand such as 2,2-bipyridine, 1,10-phenanthroline (phen) and 2,2′-biimidazole [11,17–25]. With all these compounds, concerns about molybdenum-related adverse toxicity are tempered by the knowledge that this element is essential for life and is subject to homeostatic mechanisms that maintain body levels within a narrow, healthy range [13]. Hence, it is presumed that, on the one hand, Mo-containing follow-up products (metabolites) may be relatively benign, and, on the other, the body has built-in mechanisms to process and manage them. Nevertheless, studying the chemistry of biologically active Mo complexes under physiological conditions is crucial for identifying the active species and mechanisms of action. In this direction, an important aspect of half-sandwich molybdenum carbonyl compounds is the fate of the CO ligand(s), i.e. whether they are released upon dissolution of the complexes in aqueous media. Complexes which exhibit this behavior, such as

* Corresponding author.
E-mail address: mpillinger@ua.pt (M. Pillinger).

https://doi.org/10.1016/j.ica.2026.123348
Received 1 May 2026; Received in revised form 17 June 2026; Accepted 26 June 2026
Available online 27 June 2026

[(η^5-Cp)Mo(CO)$_3$Cl] [32], are known as CO-releasing molecules (CORMs) and are interesting in their own right as prodrugs for the safe delivery of controlled amounts of CO [33–35], which is a potential therapeutic agent with vasodilatory, anti-inflammatory, antiapoptotic, bactericidal, and anti-cancer properties [36]. Due to these effects, the combined introduction of both Cp' and CO ligands on metal centers may afford complexes with multitherapeutic action as well as enhanced cytotoxicity due to synergistic effects between the [Cp'M]$^{n+}$ fragment and released CO [37,38].

In the present work, we have prepared the complexes [(η^5-Cp')Mo(CO)$_2$(en)][BF$_4$] (Cp' = Cp (**3**), Ind (C$_9$H$_7$) (**4**); en = ethylenediamine), determined the crystal structure of **4**, and studied the stability of the complexes in the solid-state and in solution, including quantification of the CO-release behavior under simulated physiological conditions, in the dark or under irradiation with visible light. These complexes are expected to have reasonable aqueous solubility due to their ionic character. We chose the en ligand because, by analogy with ruthenium(II) arene anticancer complexes of the type [(η^6-arene)Ru(II)(en)X] [39,40], the NH groups of coordinated en can potentially form H-bonds with DNA bases, thereby providing a driving force for DNA binding that could complement that provided by hydrophobic Cp'-nucleobase interactions, leading to altered profiles of biological activity.

2. Experimental section

2.1. Materials and methods

All preparations and manipulations were carried out using standard Schlenk techniques under nitrogen. The chemicals molybdenum hexacarbonyl (technical grade), allyl chloride (99%), indene (technical grade, ≥90%), sec-butyllithium solution (1.6 M in hexanes), tetrafluoroboric acid diethyl ether complex, 2.4 M sodium cyclopentadienylide (NaCp) in THF, ethylenediamine (99%), anhydrous THF (≥99.9%), acetonitrile (≥99.9%, Riedel-de Haën), anhydrous dichloromethane (≥99.8%), n-hexane (≥98.5%, Carlo Erba), and diethyl ether (≥99.8%, Riedel-de Haën) were purchased from Sigma-Aldrich (unless otherwise indicated) and used as received. The complexes [(η^5-Cp)Mo(η^3-C$_3$H$_5$)(CO)$_2$] (**1**) [41] and [(η^5-Ind)Mo(η^3-C$_3$H$_5$)(CO)$_2$] (**2**) [41,42] were prepared according to previously reported procedures. ^{1}H NMR and FT-IR (ν(CO)) data for **1** and **2** matched those reported previously for the same complexes [41,42]. For the myoglobin (Mb) assays, Mb from equine skeletal muscle (95–100%, lyophilized powder), sodium dithionite (≥82%), and phosphate buffered saline (PBS) tablet (to prepare 10 mM phosphate buffer, pH 7.4) were purchased from Sigma-Aldrich and used as received. Anhydrous dimethyl sulfoxide (99.9%, Merck) was stored over molecular sieves under a nitrogen atmosphere. The gases used in this work were carbon monoxide (≥99.0%, Sigma- Aldrich) and nitrogen (Alphagaz Nitrogen type 1, 99.9% (H$_2$O < 3 ppm, O$_2$ < 2 ppm), AirLiquide).

CHN microanalyses were obtained using a TruSpec Micro CHNS 630–200-200 elemental analyzer (Leco, Saint Joseph, MI, USA). ATR FT-IR spectra were recorded using a Bruker Tensor 27 spectrophotometer fitted with a Specac Golden Gate Mk III ATR accessory (Specac, Orpington, UK) comprising a diamond top plate and KRS-5 focusing lenses (resolution 4 cm^{-1}, 256 scans). Solution ^{1}H and ^{13}C NMR spectra were measured with a Bruker Avance III 300 MHz instrument at ambient temperature. UV–Vis spectra were collected using a GBC UV/Vis 918 Cintral spectrophotometer in the absorbance mode, in the range 450–650 nm, with a slit width of 2 nm, a scan speed of 200 nm min^{-1}, and a data interval of 0.48 nm. For the stability studies and Mb assays, irradiation with visible light (400–700 nm) was performed using an Aspire cold white LED Floodlight lamp (50 W, 6000 K, 5500 lm, 230 V, 50 Hz, 230 mA, beam angle 120°, E = 10 mW cm^{-2}).

2.2. Preparation of [(η^5-Cp')Mo(CO)$_2$(en)][BF$_4$] (Cp' = Cp (**3**), Ind (**4**))

The literature method for the preparation of [(η^5-Ind)Mo(CO)$_2$(en)][BF$_4$] (**4**) was followed and adapted accordingly for the preparation of **3** [43]. One molar equiv. of HBF$_4$·Et$_2$O was added to a stirred solution of [(η^5-Cp')Mo(η^3-C$_3$H$_5$)(CO)$_2$] (1.90 mmol for **3**; 0.89 mmol for **4**) in CH$_2$Cl$_2$ (30 mL for **3**; 15 mL for **4**) at ambient temperature, giving the adduct [(η^5-Cp')Mo(η^3-C$_3$H$_5$)(CO)$_2$(FBF$_3$)]. After 10 min, 1 molar equiv. of en was added to the resultant red solution and the reaction was left for 1 h. After concentration of the mixture by solvent evaporation under reduced pressure, the addition of n-hexane (for **3**) and/or diethyl ether (for **3** and **4**) led to the precipitation of a dark red solid, which was filtered and vacuum-dried. Data for **3**: Yield: 0.50 g, 72%. Anal. Calcd for C$_9$H$_{13}$BF$_4$MoN$_2$O$_2$ (363.96): C, 29.70; H, 3.60; N, 7.70. Found: C, 29.34; H, 3.89; N, 8.15%. Selected ATR FT-IR: ν(CO) 1949 (vs), 1835 (vs) cm^{-1}. ^{1}H NMR (300 MHz, 25 °C, Me$_2$CO-d_6): 5.85 (s, 5H, Cp), 5.17 (br, 2H, NH$_2$), 4.78 (br, 2H, NH$_2$), 2.85–2.75 (m, 2H, CH$_2$), 2.74–2.64 (m, 2H, CH$_2$) ppm. Data for **4**: Yield: 0.31 g, 83%. Anal. Calcd for C$_{13}$H$_{15}$BF$_4$MoN$_2$O$_2$ (414.01): C, 37.71; H, 3.65; N, 6.77. Found: C, 37.37; H, 3.88; N, 7.00%. Selected ATR FT-IR: ν(CO) 1960 (vs), 1850 (vs) cm^{-1}. ^{1}H NMR (300 MHz, 25 °C, Me$_2$CO-d_6): 7.87 (m, 2H, H$^{5–8}$), 7.55 (m, 2H, H$^{5–8}$), 6.28 (d, 2H, H^{1,3}), 5.24 (t, 1H, J_{H-H} = 2.8 Hz, H^2), 2.32 (m, 2H, CH$_2$), 1.70 (m, 2H, CH$_2$) ppm. ^{1}H NMR spectroscopic data for **4** agree with the literature data [43]. Single crystals of **4** suitable for X-ray diffraction were isolated by slow cooling of a concentrated solution in CH$_2$Cl$_2$.

2.3. Single crystal X-ray diffraction studies

Crystalline material of the compound [(η^5-Ind)Mo(CO)$_2$(en)][BF$_4$]·CH$_2$Cl$_2$ (**4**·CH$_2$Cl$_2$) was collected from the crystallization vial and immediately immersed in inert viscous oil. A suitable single crystal was selected and mounted on a CryoLoop with the assistance of a stereomicroscope [44]. Diffraction data sets were collected at 150(2) K on a Bruker X8 APEX II CCD area-detector diffractometer (Mo K$_\alpha$ graphite-monochromated radiation, λ = 0.71073 Å) controlled by the APEX2 software package [45] and equipped with an Oxford Cryosystems Series 700 cryostream cooler. Images were processed using SAINT+ [46], and absorption effects were corrected by the multi-scan semi-empirical method implemented in SADABS [47]. The structures were solved using the algorithms implemented in SHELXT-2014 [48,49], allowing the direct location of almost all the heaviest atoms. The remaining non-H atoms were located from difference Fourier maps calculated from successive full-matrix least squares refinement cycles on F^2 using SHELXL-v.2019 [48,50], and all of them were successfully refined using anisotropic displacement parameters.

H-atoms bound to carbon were located at model geometrical positions using suitable HFIX instructions in SHELXL: *43* for the aromatic and *23* for the –CH$_2$– groups belonging to the ligands or CH$_2$Cl$_2$ molecule of crystallization. All these atoms were included in subsequent refinement cycles in riding-motion approximation with isotropic thermal displacement parameters (U_{iso}) fixed at 1.2 × U_{eq} of the attached carbon atom. H-atoms of the amine groups of the en ligand were markedly visible in the difference Fourier maps, and included in subsequent refinement stages with the N−H distances restrained to ensure a chemically reasonable geometry for these groups.

Table S1 in the Supporting Information summarizes relevant information about the crystal data, single crystal X-ray data collection and structure refinement details. CCDC 2550579 contains the supplementary crystallographic data for this paper. These data can be obtained free of charge via https://www.ccdc.cam.ac.uk/structures/.

2.4. Stability studies

To evaluate the stability of the complexes in solution, 4 mM solutions were freshly prepared in degassed DMSO (for complexes **1** and **2**) or

degassed 10 mM PBS, pH 7.4 (for complexes **3** and **4**), and then diluted to 100–500 μM, depending on the molar absorptivity of the complexes. To mimic the conditions of the myoglobin (Mb) assay, the solutions were incubated at 37 °C with constant magnetic stirring, in the dark or under irradiation with visible light (E = 10 mW cm^{-2}), and either in the absence (capped cuvette – only for the experiment performed in the dark) or presence (uncapped cuvette) of air. Over a 6 h incubation period, the assays were interrupted in intervals of 1 h to measure the UV–Vis absorption spectra.

2.5. CO release studies using the Mb assay

CO release profiles for complexes **1**–**4** were obtained using the standard Mb assay. This spectrophotometric method was performed by monitoring the Q-band region (540–580 nm). Specifically, the conversion of deoxy-myoglobin (deoxy-Mb) to carbonmonoxy-Mb (MbCO), in which CO is bound to the iron metal center of the heme group, is tracked through the loss of the deoxy-Mb band (λ_{max} = 557 nm) and the successive growth of two new bands with λ_{max} = 540 and 577 nm that are due to MbCO.

Stock solutions of Mb (100 μM) and sodium dithionite (20 mg mL^{-1}) were freshly prepared in N_2-degassed 10 mM PBS (pH 7.4). Under an inert atmosphere, these stock solutions were added to a quartz cuvette in the following order: 10 mM PBS (1185 μL), 100 μM Mb (1500 μL) and 20 mg mL^{-1} sodium dithionite (300 μL). An initial UV–Vis absorption spectrum of the sample was measured to obtain the profile of deoxy-Mb. After that, a 15 μL aliquot of a freshly prepared 4 mM solution of **1** or **2** in N_2-degassed DMSO, or **3** or **4** in 10 mM PBS, was added to the cuvette, giving a final concentration of 20 μM. The sample was then incubated at 37 °C under constant magnetic stirring, either in the dark or under irradiation with cold white light. UV–Vis absorption spectra were measured in intervals of 15 min up to 90 min followed by intervals of 30 min up to 6 h. At the end of each assay, CO gas was bubbled through the solution in the cuvette to completely convert deoxy-Mb to MbCO, and then the spectrum of MbCO was measured. This allowed the actual concentration of Mb in the cell ([Mb] = 40–50 μM) to be determined, using the known extinction coefficient of MbCO at 540 nm (15.4 mM^{-1} cm^{-1}) [51]. The assays were carried out in duplicate or triplicate, and the spectroscopic data were treated in the standard way by applying a correction at the 510 nm isosbestic point [52].

3. Results and discussion

3.1. Synthesis and characterization

The complexes [(η^5-Cp')Mo(CO)$_2$(en)][BF$_4$] (Cp' = Cp (**3**), Ind (**4**)) were prepared by the well-established method [41,43] in which the starting η^3-allyl complexes [(η^5-Cp')Mo(η^3-C$_3$H$_5$)(CO)$_2$] (Cp' = Cp (**1**), Ind (**2**)) are protonated with HBF$_4$·Et$_2$O in CH_2Cl_2 to give the η^2-propene compounds [(η^5-Cp')Mo(η^2-C$_3$H$_6$)(CO)$_2$(FBF$_3$)], and the resultant red solutions are then treated with en to give **3** and **4** (Scheme 1). The cations in **3** and **4** were described previously: as the PF_6 salt in ref. [53] for Cp' = Cp, and as the BF_4 salt in ref. [43] for Cp' = Ind. Compounds **3** and **4** present very different solubilities compared to their starting η^3-allyl complexes **1** and **2**, which are insoluble in water. **3** and **4** are soluble in polar solvents but insoluble in apolar solvents (like n-hexane and diethyl ether); in chlorinated solvents, **3** and **4** are only sparingly soluble. In the solid-state, **3** and **4** are air-stable, with no measurable alterations occurring in the ATR FT-IR spectra of solids exposed to air for up to 8 days (Fig. S1 in the Supporting Information).

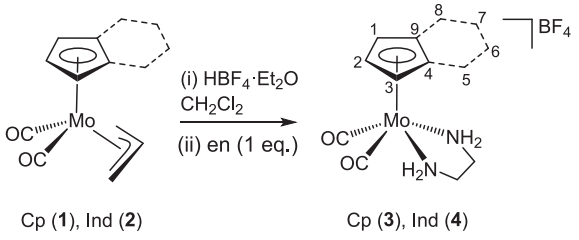

Scheme 1. Synthesis of compounds **3** and **4**.

The ATR FT-IR spectra of **3** and **4** are quite similar in the frequency range of 800–3500 cm^{-1} (Fig. 1). Selected assignments are given in Table 1. As expected for cationic dicarbonyl complexes of the type [(η^5-Cp')Mo(CO)$_2$(L)]$^+$, the spectra show two very strong bands in the terminal carbonyl stretching region (bands at 1835 and 1949 cm^{-1} for **3**, 1850 (with a shoulder at 1833 cm^{-1}) and 1960 cm^{-1} for **4**; the average ν(CO) values are 1892 cm^{-1} for **3** and 1900 cm^{-1} for **4**). The shift to higher frequency of the ν(CO) bands (compared with those for **1** (1823, 1917 cm^{-1}) and **2** (1840, 1925 cm^{-1})) is consistent with the cationic nature of **3** and **4**. A band with medium intensity at 430 cm^{-1} for **3** and 440 cm^{-1} for **4** is assigned to an asymmetric Mo—C stretching vibration [54]. Hence, the ν(CO) and ν_{asym}(Mo—C) frequencies are little affected by replacement of the η^5-cyclopentadienyl ligand by the η^5-indenyl ligand, which suggests that the coordination strength of the CO groups is quite similar in the two complexes. This has been documented for related Cp/Ind complexes such as [(η^5-Cp')Mo(CO)$_2$(phen)][BF$_4$] [18]. The appearance of a resolved shoulder on the lower-frequency ν(CO) band for **4** is attributed to solid-state (crystal packing) and vibrational coupling effects. Bands for coordinated en in **3** (1593, 3293 and 3345 cm^{-1}) and **4** (1589, 3288 and 3331 cm^{-1}) are slightly shifted with respect to the corresponding bands for the free ligand (NH_2 deformation mode at 1597 cm^{-1}; N—H stretching vibrations at 3280 and 3355 cm^{-1}).

The molecular structure of complex **4** was determined by single crystal X-ray diffraction. Complex **4** crystallized in the orthorhombic space group *P*bca with one molecule of **4** and one molecule of dichloromethane in the asymmetric unit (Fig. 2). The cationic complex reveals a single Mo center with distorted square-pyramidal molecular geometry resulting from the coordination to two cis-arranged carbonyls and two nitrogen donors of en (in the basal plane), as well as the η^5 coordination mode of the C5 ring of the indenyl ligand in the apical position. The bidentate en ligand is located below the annulated benzene ring of the indenyl, representing the most common conformation of

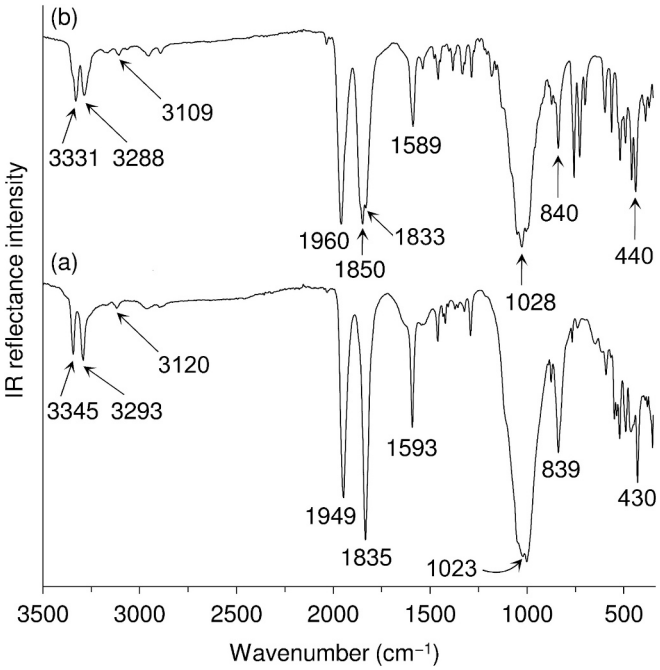

Fig. 1. ATR FT-IR spectra of (a) **3** and (b) **4**.

Table 1.
Selected IR bands and assignments for complexes **3** and **4**.

3	4	Assignment[a]
3345	3331	ν(N—H), en
3293	3288	ν(N—H), en
3120	3109	ν(C—H), Cp'
1949	1960	ν_s(C≡O)
1835	1850/1833	ν_{as}(C≡O)
1593	1589	δ(N—H), en
1023	1028	ν(B—F), $[BF_4]^-$ (+β(C—H), Cp')
839	840	γ(C—H), Cp'
430	440	ν_{as}(Mo—C)

[a] Based on the complete assignment of the vibrational modes of [CpMo$(CO)_3$R]-type complexes [54].

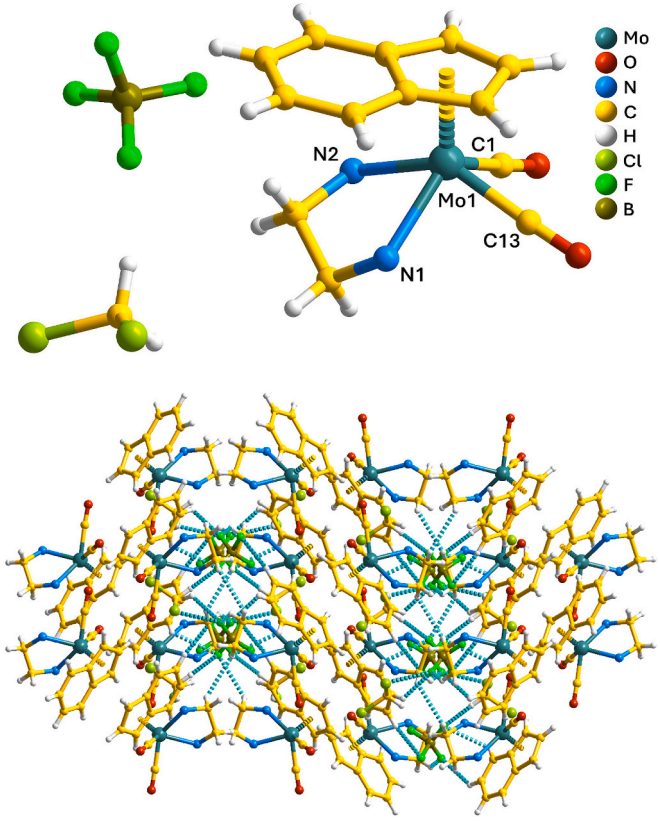

Fig. 2. (top) Crystal structure of [(η^5-Ind)Mo$(CO)_2$(en)][BF_4]·CH_2Cl_2 (**4**·CH_2Cl_2) showing the labelling scheme for all atoms composing the Mo coordination environment (Mo1−*Cg*(η^5-Ind), 2.013(3) Å; Mo1−C1, 1.936(3) Å; Mo1−C13, 1.971(3) Å; Mo1−N1, 2.274(2) Å; Mo1−N2, 2.270(2) Å); (bottom) Extended crystal packing features of the complex, with most of the C—H···F interactions drawn as dashed turquoise lines (viewed in the 100 direction of the unit cell). Hydrogens attached to N1 and N2 have been omitted for clarity. (For interpretation of the references to colour in this figure legend, the reader is referred to the web version of this article.)

indenyl complexes of the type [(η^5-Ind)Mo$(CO)_2$(^{NN}L)]$^+$ reported for various chelates [18,20,23]. This conformation aligns with Faller's rule of thumb [55], which states that the benzene ring of the indenyl group will be trans to the ligand with the highest trans effect (CO). The Mo—N (en) bond distances [Mo1−N1 = 2.274(2) Å and Mo1−N2 = 2.270(2) Å] are intermediate between those typically observed for octahedral complexes of the type [Mo$(CO)_2$(η^3-C_3H_5)(en)X] (X=Br, N_3, $NCBH_3$) in which one of the donor atoms of the bidentate ligand is in the axial position and trans- to the allyl group (Mo−N = 2.245–2.248 Å), and the other is in the equatorial position and trans- to a carbonyl (Mo−N = 2.286–2.295 Å) [56,57]. As the trans-effect of the carbonyl ligands is weaker for the square pyramidal coordination geometry vs. the octahedral one, the Mo—N bond distances for the former are slightly shorter than the Mo—N(equatorial) distances for the latter. The extended crystal packing of **4**·CH_2Cl_2 is mediated by an extensive network of weak C—H···F hydrogen bonds (dashed turquoise lines in Fig. 2, bottom). The existence of the CH_2Cl_2 solvent molecule of crystallization and the cooperative effect of the extensive hydrogen bonding network, lead to considerably compact packing arrangements with the absence of channels or voids.

3.2. Stability and CO release studies

Prior to performing CO release studies, the stability of complexes **3** and **4** under simulated physiological conditions was evaluated by UV–Vis absorption spectroscopy. Solutions of **3** (350 μM) or **4** (100 μM) in degassed 0.01 M PBS (pH 7.4) were freshly prepared and then kept at 37 °C either in the dark under air, in the dark under N_2, or under N_2 with constant exposure to cold white light (400–700 nm, E = 10 mW cm^{-2}). Fig. 3 shows the development of the UV–Vis spectra over a period of 6 h; Fig. S2 and S3 in the Supporting Information compare in the same plot the spectra obtained for **3** or **4** at 0 h and at 6 h for the three different conditions, and Fig. S4 shows absorbance-time plots at selected wavelengths. The spectra obtained at 0 h for complexes **3** and **4** (plotted together in Fig. S5 as molar absorptivity versus wavelength) display a strong absorption below 280 nm that is tentatively assigned to metal-to-ligand charge-transfer (MLCT) and/or Cp'-centered π–π* transitions [58–60]. A resolved shoulder at 247 nm for complex **4** is assigned (in accordance with the molar absorptivity of 11,800 M^{-1} cm^{-1}) to MLCT transitions involving Mo dπ orbitals and CO/indenyl π* orbitals [61–65]. The same assignment applies to the less intense low-energy shoulder near 280 nm (extending to 360 nm). The corresponding feature for **3** extends to lower energy (400 nm) and is composed of several overlapping bands, with the lowest energy one being centered near 330 nm. A previous study that compared the electronic properties and photochemistry of the rhodium dicarbonyl derivatives [(η^5-Cp)Rh$(CO)_2$] and [(η^5-Ind)Rh$(CO)_2$] highlighted the fact that the π–π* band for the latter is substantially red-shifted due to the increased conjugation of the indenide group [60]. Hence, in analogy with that discussed for [(η^5-Ind)Rh$(CO)_2$], in complex **4** there could be significant overlap by the π–π* states in the lower-energy region of the spectrum, at least up to 350 nm. Both **3** and **4** display a weak and broad band, with a low-energy shoulder, in the visible region centered at ~430 nm for **3** (ε = 300 M^{-1} cm^{-1}) and 415 nm for **4** (ε = 630 M^{-1} cm^{-1}), which is assigned to MLCT and/or (because the molar extinction coefficient is relatively low (10–10^3 M^{-1} cm^{-1}) [66]) ligand field (LF) transitions [31,63,67]. This assignment is backed up by DFT calculations that were performed to understand the UV–Vis spectra and redox behavior of [(η^5-Ind)Mo$(CO)_2$(α-diimine)]$^+$ cations [68]. Bands near 400 nm for a model compound containing a diazabutadiene ligand were partially attributed to metal-centered transitions (d-d and metal to CO and indenyl). For **3** and **4**, a combination of DFT/TD-DFT calculations and solvatochromic studies may be needed to distinguish MLCT bands from ligand-centered (π–π*) and d-d (LF) absorptions.

For the solutions of **3** and **4** stored under N_2 in the dark, a relatively slow, gradual loss of absorbance was observed in the wavelength range between 210 and 700 nm (Fig. 3b, e and S4), which may be associated with degradation of the complexes. No new absorption bands are observed. For complex **3**, irradiation of the solution with visible light (under N_2) leads to only a small change in the spectral series, with a slightly faster loss of absorbance at longer irradiation times (4–6 h, Fig. 3c and S4a). On the other hand, the decay is noticeably faster for complex **4**, with 3 h of illumination leading to complete loss of the absorption peak at 415 nm, and reduction of the peak at 247 nm to an unresolved shoulder (Fig. 3f and S4b). The relative loss of absorbance in the peaks at 247, ~287 and 415 nm is faster still for the solution exposed to air in the dark, with loss of the band in the visible region after 2 h

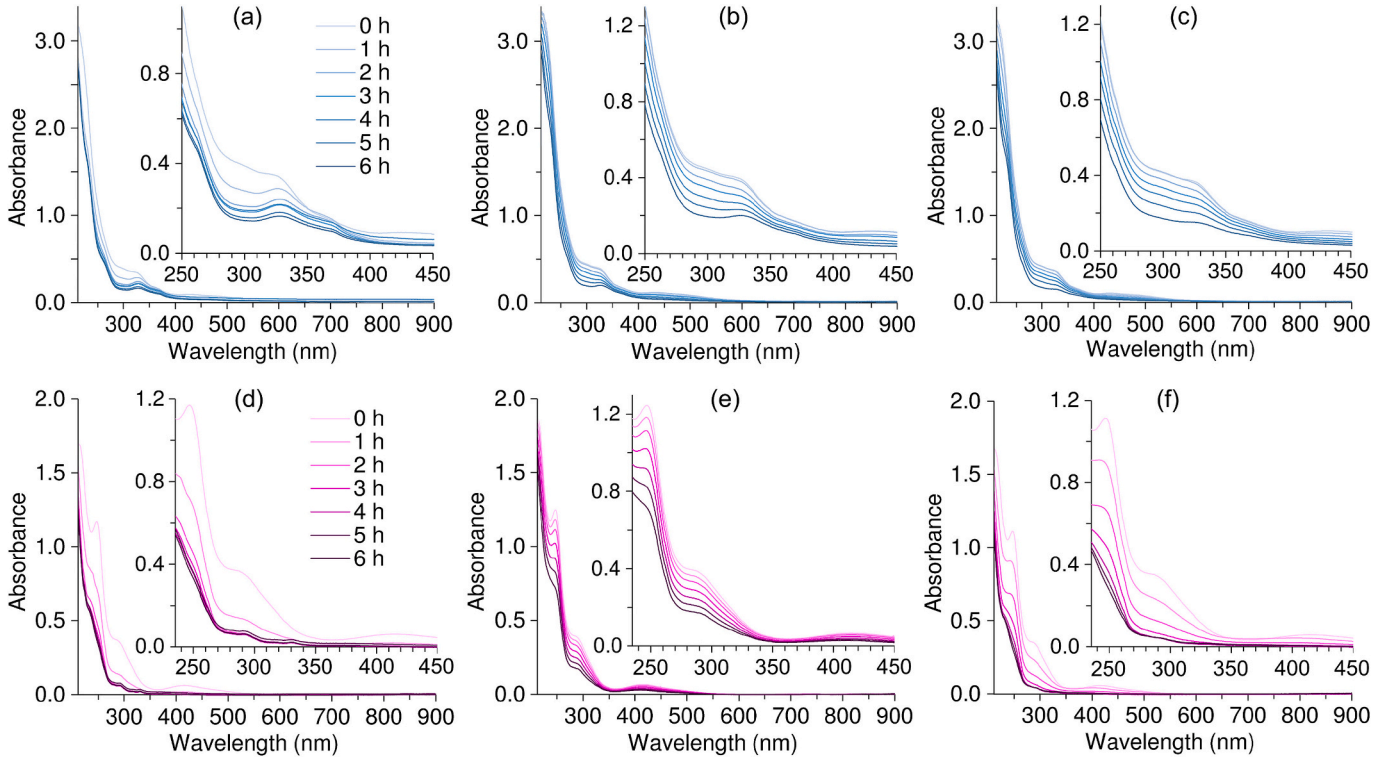

Fig. 3. UV–Vis absorption spectra recorded over a period of 6 h for solutions of (a–c) **3** (350 μM) and (d–f) **4** (100 μM) in 0.01 M PBS (pH 7.4) that were kept at 37 °C either in the dark under air (a, d), in the dark under N_2 (b, e), or under N_2 with constant exposure to cold white light (c, f).

(Fig. 3d and S4b). The spectrum obtained after 6 h is similar to that obtained after the same time for the illuminated solution except that the former shows two new, very weak bands with λ_{max} at 291 and 330 nm (Fig. S3). In a similar fashion, the exposure of the solution of **3** to air in the dark (Fig. 3a) leads to a spectrum that is similar to that obtained under N_2 (Fig. 3b) except for the growth of a shoulder near 370 nm (Fig. S2). While the origin of these new bands between 290 and 370 nm remains unclear, they may be tentatively attributed to $O^{2-} \rightarrow Mo^{6+}$ (d^0) ligand-to-metal charge transfer transitions (in Mo═O and/or Mo—O—Mo bonds) [69], which would be suggestive of an oxidative decarbonylation process.

The ability of complexes **1–4** to release CO under physiologically relevant conditions (10 mM PBS, pH 7.4, 37 °C) was assessed using the myoglobin-based aqueous assay. Here, the CO liberated by a complex is captured by deoxymyoglobin (deoxy-Mb) to afford carbonmonoxymyoglobin (MbCO), and this conversion may be quantified by following changes in the Q-band region of the electronic absorption spectrum of Mb. Solutions of **1**–**4** with a final concentration of 20 μM were evaluated. DMSO was used as the delivery solvent for **1** and **2**, while 10 mM PBS was used for **3** and **4**. No changes in the Q-band region were observed for the assays performed over 6 h with the allyl complexes **1** and **2**, indicating that these complexes are stable in DMSO-water buffered solutions (Fig. S6 in the Supporting Information). In contrast, **3** and **4** were able to convert deoxy-Mb to MbCO, albeit relatively slowly as shown by the CO release profiles (Fig. 4); selected assay data (visible absorption spectra and corresponding difference spectra) are given in Fig. S7. Complex **3** released CO very slowly with an initial rate (up to 60 min) of ca. 0.015 μM min^{-1}. CO liberation continued very slowly after 60 min, almost reaching a plateau after 6 h, with the total CO release being 3.34 ± 0.03 μM, corresponding to 0.17 molecules of CO per molecule of **3**. CO release from **4** was significantly faster, with an initial rate of ca. 0.09 μM min^{-1} and a final MbCO concentration at 6 h of 14.7 ± 0.8 μM, corresponding to 0.74 equivalents. These results align with the stability studies conducted without protein (Fig. 3b and e), which showed progressive loss of bands and therefore decomposition of

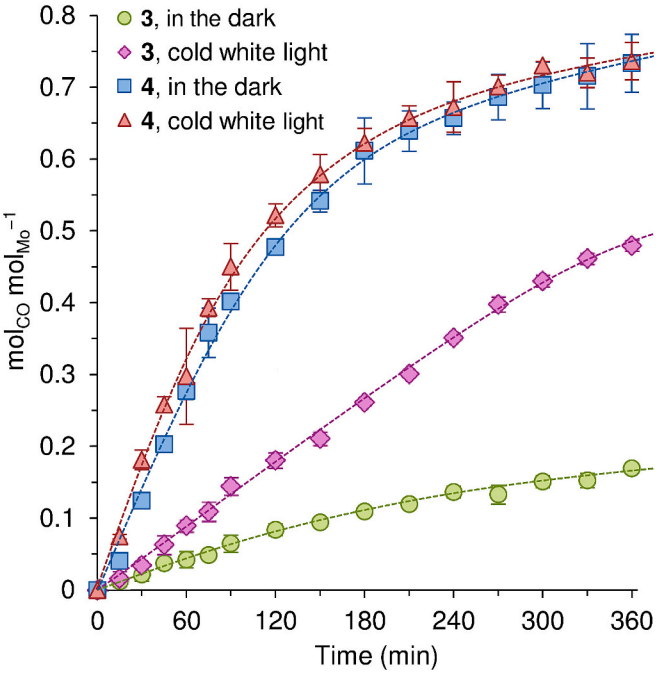

Fig. 4. CO release profiles determined from Mb assays performed at 37 °C with 20 μM solutions of **3** and **4**, either in the dark or with visible-light irradiation. The data values are the mean ± standard deviation of 2 or 3 independent assays.

the complexes over time. The CO release profile for **4** indicates a half-life, $t_{1/2}$, of 129 ± 10 min (defined as the time taken to produce an MbCO concentration of 10 μM). This positions complex **4** as a slow CO releaser in the context of other "spontaneous" Mo-based CORMs that

liberate CO upon incubation in buffered aqueous solutions at 37 °C. For example, cyclopentadienyl $[CpMo(CO)_3Cl]$ (20 μM) and $[CpMo(CO)_3(\eta^1$–2-pyrone)] (40 μM) complexes exhibited half-lives of 11.4 and 14.4 min, respectively, for CO release in the dark [29,32].

Photochemical promotion of CO release from $[CpMo(CO)_3R]$ complexes has been reported in a few cases. The complexes with R = Me [70] and $C{\equiv}CCH_2OR'$ (R′ = β-D-fructopyranose) [32] showed enhanced CO release under UV irradiation (325–365 nm), whereas, to the best of our knowledge, the complex with R = η^1-*N*-imidato is the only half-sandwich Mo-CORM reported to date to release CO upon visible-light illumination (450–650 nm) [71]. Although the UV light-induced release of CO is a general reaction of metal carbonyl complexes, such short wavelengths are poorly suited for biomedical applications, where visible or near-infrared light is preferred due to deeper tissue penetration and reduced phototoxicity [72]. Given that CO release from **3** was very low under thermal conditions, the possibility of using visible-light irradiation to promote CO release was investigated. Mb assays with **3** (final concentration 20 μM) were conducted as before but with exposure to cold white light (as performed in the stability studies). This resulted in a more rapid and significant release of CO when compared with the dark reaction, with a half-life of 380 ± 15 min (Fig. 4). CO was released steadily for 5 h, showing the potential for sustained photodecarbonylation. Complex **4**, in contrast, did not exhibit enhanced CO release upon irradiation with visible light (Fig. 4). The capacity of **3** to undergo enhanced CO liberation under illumination with visible light may be explained, at least in part, by the slightly more pronounced extension of its UV–Vis absorption tail into the visible region ($\lambda > 500$ nm) relative to **4** (Fig. S5 in the Supporting Information), and different relative contributions of LF and Mo → CO MLCT transitions to the lowest-energy ($\lambda > 350$ nm) absorptions [60]. With the LED lamp used, only the visible band at ~430 nm is excited, i.e., the transitions in the UV region are not populated. In future mechanistic studies, it may be helpful to combine the aforementioned DFT/TD-DFT calculations and solvatochromic experiments with an Investigation of the wavelength dependence of photoreactivity, i.e., Mb assays performed using narrow bandwidth radiation covering the UV and visible range. UV irradiation may give qualitatively different CO-release profiles for **3** and **4**. Considering the interpretation of analogous behavior observed for the complexes $[(\eta^5$-Cp)$Rh(CO)_2]$ and $[(\eta^5$-Ind)$Rh(CO)_2]$ [60], there are other factors that could contribute to the observed inertness of **4** toward photodecarbonylation under longer-wavelength (visible) light irradiation, including the increased ability of the indenyl ligand to undergo $\eta^5 \rightarrow \eta^3$ ring slippage, and the existence of additional vibrational deactivation modes from the LF excited states.

The CO photorelease results show no obvious correlation with the stability studies conducted without Mb, where the data indicate that complex **4** undergoes faster decomposition than complex **3** upon visible-light irradiation (Fig. 3c and f, Fig. S4). Concentration effects could be a factor, since the Mb assays were performed with 20 μM solutions, while the stability studies were performed with concentrations of 350 μM for **3** and 100 μM for **4**. At higher concentrations, complex **4** or its CO-depleted form may be more susceptible to aggregation (owing to the propensity of indenyl ligands to form stacking interactions that are significantly stronger than those possible with cyclopentadienyl ligands), which could promote ligand-centered photodegradation. A different explanation can be proposed by considering how the Cp and Ind ligands bias the system toward divergent thermal and photochemical pathways. For complex **4**, associative substitution and hence thermal CO release (i.e., in the dark) could be made easier by ring slippage (the classic *indenyl effect*). Once CO loss has occurred, however, the resulting product appears to be far more photoreactive than the Cp analogue: under visible-light irradiation, the lowest-energy excited states of the Ind system seem to favor rapid decomposition (e.g., hydrolysis) rather than further productive CO dissociation, leading to rapid bleaching of the UV–vis spectrum. In contrast, under visible light, the Cp complex **3** may access MLCT or metal-centered excited states that are reasonably efficient at promoting selective CO dissociation but do not strongly predispose the remaining fragment to rapid decomposition, consistent with its enhanced CO release and greater photostability.

4. Conclusions

In summary, two cationic half-sandwich molybdenum(II) dicarbonyl complexes bearing ethylenediamine, $[(\eta^5$-Cp)$Mo(CO)_2$(en)$][BF_4]$ (**3**) and $[(\eta^5$-Ind)$Mo(CO)_2$(en)$][BF_4]$ (**4**), were synthesized and characterized, with the structure of **4** confirmed by single-crystal X-ray diffraction. Both complexes display good solid-state stability and enhanced solubility in polar media, but undergo gradual decomposition in aqueous solution under physiological conditions, with rates modulated by ligand identity, oxygen, and visible-light irradiation. Myoglobin assays demonstrate that, unlike their η^3-allyl precursors, both compounds behave as CO-releasing molecules, albeit with slow release profiles. The indenyl derivative **4** exhibits significantly faster and more extensive CO release under thermal conditions, whereas the cyclopentadienyl analogue **3** shows limited thermal CO liberation but enhanced release upon visible-light irradiation, highlighting its potential as a photoactivatable CORM. Overall, the results underline the important role of the Cp' ligand in modulating both stability and CO-release behavior, and support the continued exploration of such systems as multifunctional platforms combining organometallic cytotoxicity with controlled CO delivery.

CRediT authorship contribution statement

Sofia M. Bruno: Methodology, Validation, Formal analysis, Investigation, Writing – original draft, Writing – review & editing, Supervision. **Isabel B. Calhau:** Methodology, Validation, Investigation, Writing – review & editing. **Tiago M. Dias:** Validation, Investigation, Writing – original draft. **Adriana Santos:** Validation, Investigation, Writing – original draft. **Luís Cunha-Silva:** Formal analysis, Investigation, Writing – original draft, Visualization. **Mariela M. Nolasco:** Validation, Investigation, Writing – original draft. **Isabel S. Gonçalves:** Conceptualization, Resources, Writing – original draft, Supervision, Project administration, Funding acquisition.**Martyn Pillinger:** Conceptualization, Resources, Writing – original draft, Writing – review & editing, Visualization, Supervision, Funding acquisition.

Declaration of competing interest

The authors declare that they have no known competing financial interests or personal relationships that could have appeared to influence the work reported in this paper.

Acknowledgments

This work was developed within the scope of the strategic projects for CICECO – Aveiro Institute of Materials [UID/50011/2025 (DOI 10.54499/UID/50011/2025) & LA/P/0006/2020 (DOI 10.54499/LA/P/0006/2020)] and Laboratório Associado para a Química Verde - Tecnologias e Processos Limpos [LAQV/REQUIMTE - UID/50006/2025 (DOI 10.54499/UID/50006/2025], and the "RemovCO2" R&D Exploratory Project 2024.17214.PEX (DOI 10.54499/2024.17214.PEX), all financed by national funds through the FCT (Fundação para a Ciência e a Tecnologia) / MECI (Ministério da Educação, Ciência e Inovação) (PIDDAC). We acknowledge funding provided by the Innovation and Digital Transition Program (COMPETE 2030), in its European Regional Development Fund (ERDF) component, through the project with ref. COMPETE2030-FEDER-00782200 (FCT ref. 16641). I.B.C. (ref. 2021.05953.BD, DOI 10.54499/2021.05953.BD) thanks the FCT and the European Social Fund for a PhD grant. The NMR spectrometers are part of the National NMR Network (PTNMR) and are partially supported by Infrastructure Project No. 022161 (co-financed by FEDER through

COMPETE 2020, POCI and PORL and FCT through PIDDAC).

Appendix A. Supplementary data

Supplementary data to this article can be found online at https://doi.org/10.1016/j.ica.2026.123348.

Data availability

Data will be made available on request.

References

[1] P.M. Abeysinghe, M.M. Harding, Antitumour bis(cyclopentadienyl) metal complexes: titanocene and molybdocene dichloride and derivatives, Dalton Trans. (2007) 3474–3482, https://doi.org/10.1039/B707440A.

[2] E. Meléndez, Bioorganometallic chemistry of molybdenocene dichloride and its derivatives, J. Organomet. Chem. 706-707 (2012) 4–12, https://doi.org/10.1016/j.jorganchem.2012.02.006.

[3] P. Köpf-Maier, M. Leitner, R. Voigtländer, H. Köpf, Molybdocene dichloride as an antitumor agent, Z. Naturforsch. 34C (1979) 1174–1176, https://doi.org/10.1515/znc-1979-1215.

[4] J.B. Waern, C.T. Dillon, M.M. Harding, Organometallic anticancer agents: cellular uptake and cytotoxicity studies on thiol derivatives of the antitumor agent molybdocene dichloride, J. Med. Chem. 48 (2005) 2093–2099, https://doi.org/10.1021/jm049585o.

[5] I. Feliciano, J. Matta, E. Meléndez, Water-soluble molybdenocene complexes with both proliferative and antiproliferative effects on cancer cell lines and their binding interactions with human serum albumin, J. Biol. Inorg. Chem. 14 (2009) 1109–1117, https://doi.org/10.1007/s00775-009-0554-0.

[6] X. Narváez-Pita, C. Ortega-Zuniga, C.Y. Acevedo-Morantes, B. Pastrana, J. Olivero-Verbel, W. Maldonado-Rojas, J.E. Ramírez-Vick, E. Meléndez, Water soluble molybdenocene complexes: synthesis, cytotoxic activity and binding studies to ubiquitin by fluorescence spectroscopy, circular dichroism and molecular modeling, J. Inorg. Biochem. 132 (2014) 77–91, https://doi.org/10.1016/j.jinorgbio.2013.10.014.

[7] W. Kandioller, M. Reikersdorfer, S. Theiner, A. Roller, M. Hejl, M.A. Jakupec, M. S. Malarek, B.K. Keppler, The impact of leaving group variation on the anticancer activity of molybdenocenes, Organometallics 37 (2018) 3909–3916, https://doi.org/10.1021/acs.organomet.8b00582.

[8] V. Fuchs, K. Cseh, M. Hejl, P. Vician, B. Neuditschko, S.M. Meier-Menches, L. Janker, A. Bileck, N. Gajic, J. Kronberger, M. Schaier, S. Neumayer, G. Köllensperger, C. Gerner, W. Berger, M.A. Jakupec, M.S. Malarek, B.K. Keppler, Highly cytotoxic molybdenocenes with strong metabolic effects inhibit tumour growth in mice, Chem. Eur. J. 29 (2013) e202202648, https://doi.org/10.1002/chem.202202648.

[9] B. Gleeson, J. Claffey, A. Deally, M. Hogan, L.M.M. Méndez, H. Müller-Bunz, S. Patil, M. Tacke, Novel benzyl-substituted molybdocene anticancer drugs, Inorg. Chim. Acta 363 (2010) 1831–1836, https://doi.org/10.1016/j.ica.2010.02.020.

[10] L.Y. Kuo, M.G. Kanatzidis, M. Sabat, A.L. Tipton, T.J. Marks, Metallocene antitumor agents. Solution and solid-state molybdenocene coordination chemistry of DNA constituents, J. Am. Chem. Soc. 113 (1991) 9027–9045, https://doi.org/10.1021/ja00024a002.

[11] M.R.P. Norton de Matos, C.C. Romão, C.C.L. Pereira, S.S. Rodrigues, M. Mora, M.J. P. Silva, P.M. Alves, C.A. Reis, Compositions comprising organometallic molybdenum compounds for treating cancer, International patent WO/2005/087783, 2005.

[12] M.S. Saraiva, S. Quintal, F.C.M. Portugal, T.A. Lopes, V. Félix, J.M.F. Nogueira, M. Meireles, M.G.B. Drew, M.J. Calhorda, Nitrogen donor ligands bearing N–H groups: effect on catalytic and cytotoxic activity of molybdenum η^3-allyldicarbonyl complexes, J. Organomet. Chem. 693 (2008) 3411–3418, https://doi.org/10.1016/j.jorganchem.2008.08.001.

[13] D. Bandarra, M. Lopes, T. Lopes, J. Almeida, M.S. Saraiva, M. Vasconcellos-Dias, C. D. Nunes, V. Félix, P. Brandão, P.D. Vaz, M. Meireles, M.J. Calhorda, Mo(II) complexes: a new family of cytotoxic agents? J. Inorg. Biochem. 104 (2010) 1171–1177, https://doi.org/10.1016/j.jinorgbio.2010.07.006.

[14] S. Quintal, M.J. Pires da Silva, S.R.M. Martins, R. Sales, V. Félix, M.G.B. Drew, M. Meireles, A.C. Mourato, C.D. Nunes, M.S. Saraiva, M. Machuqueiro, M. J. Calhorda, Molybdenum(II) complexes with *p*-substituted BIAN ligands: synthesis, characterization, biological activity and computational study, Dalton Trans. 48 (2019) 8449–8463, https://doi.org/10.1039/c9dt00469f.

[15] L. Šebestová, R. Havelek, M. Řezáčová, J. Honzíček, Z. Kročová, J. Vinklárek, Study of antitumor effect of selected vanadium and molybdenum organometallic complexes in human leukemic T-cells, Chem.-Biol. Int. 242 (2015) 61–70, https://doi.org/10.1016/j.cbi.2015.09.017.

[16] H. Pfeiffer, M. Dragoun, A. Prokop, U. Schatzschneider, Biological activity of molybdenum(II) allyl dicarbonyl complexes with N-N coligands of variable aromatic surface area on adherent and nonadherent human cancer cells, Z. Anorg. Allg. Chem. 639 (2013) 1568–1576, https://doi.org/10.1002/zaac.201300055.

[17] C.C.L. Pereira, C.V. Diogo, A. Burgeiro, P.J. Oliveira, M.P.M. Marques, S.S. Braga, F.A.A. Paz, M. Pillinger, I.S. Gonçalves, Complex formation between heptakis(2,6-di-*O*-methyl)-β-cyclodextrin and cyclopentadienyl molybdenum(II) dicarbonyl complexes: structural studies and cytotoxicity evaluations, Organometallics 27 (2008) 4948–4956, https://doi.org/10.1021/om800413w.

[18] J. Honzíček, J. Vinklárek, Z. Padělková, L. Šebestová, K. Foltánová, M. Řezáčová, The effect of substitution on the cytotoxicity of molybdenum(II) and tungsten(II) compounds, J. Organomet. Chem. 716 (2012) 258–268, https://doi.org/10.1016/j.jorganchem.2012.07.011.

[19] J. Honzíček, J. Vinklárek, M. Erben, Z. Padělková, L. Šebestová, M. Řezáčová, Tetrafluoro-4-pyridyl substituted cyclopentadienyl molybdenum(II) compounds, J. Organomet. Chem. 749 (2014) 387–393, https://doi.org/10.1016/j.jorganchem.2013.10.034.

[20] O. Mrózek, L. Šebestová, J. Vinklárek, M. Řezáčová, A. Eisner, Z. Růžičková, J. Honzíček, Highly water-soluble cyclopentadienyl and indenyl molybdenum(II) complexes – second generation of molybdenum-based cytotoxic agents, Eur. J. Inorg. Chem. 2016 (2016) 519–529, https://doi.org/10.1002/ejic.201501133.

[21] I. Honzíčková, J. Vinklárek, Z. Růžičková, M. Řezáčová, J. Honzíček, Modified cyclopentadienyl molybdenum compounds with enhanced cytotoxic activity towards MOLT-4 leukaemia cells, Appl. Organomet. Chem. 31 (2017) e3759, https://doi.org/10.1002/aoc.3759.

[22] J. Schejbal, L. Melounková, J. Vinklárek, M. Řezáčová, Z. Růžičková, I. Císařová, J. Honzíček, Cyclopentadienyl molybdenum(II) compounds bearing carboxylic acid functional group, Inorg. Chim. Acta 479 (2018) 66–73, https://doi.org/10.1016/j.ica.2018.04.032.

[23] O. Mrózek, L. Melounková, L. Dostál, I. Císařová, A. Eisner, R. Havelek, E. Peterová, J. Honzíček, J. Vinklárek, Enhanced cytotoxicity of indenyl molybdenum(II) compounds bearing a thiophene function, Dalton Trans. 48 (2019) 11361–11373, https://doi.org/10.1039/C9DT01698H.

[24] M. Absolonová, L. Melounková, J. Vinklárek, J. Honzíček, L. Dostál, O. Mrózek, Cyclopentadienyl-based anticancer drugs: improvement of cytotoxic activity through functionalisation of the π ligand, ChemMedChem 16 (2021) 1805–1813, https://doi.org/10.1002/cmdc.202100060.

[25] L. Hanzl, J. Vinklárek, J. Honzíček, L. Dostál, I. Císařová, L. Šacherlová, A. Eisner, D. Muthná, M. Řezáčová, Cyclopentadienyl molybdenum(II) compounds bearing ether and thioether functions in the side chain: synthesis, characterization, and cytotoxic/cytostatic studies, ChemPlusChem 88 (2023) e202300374, https://doi.org/10.1002/cplu.202300374.

[26] S.X. Lee, C.H. Tan, W.L. Mah, R.C.S. Wong, Y.L. Cheow, K.S. Sim, K.W. Tan, Synthesis of group 6 (chromium, molybdenum, and tungsten) photoCORMs as potential antimicrobial and anticancer agents, Inorg. Chim. Acta 525 (2021) 120491, https://doi.org/10.1016/j.ica.2021.120491.

[27] S.X. Lee, C.H. Tan, W.L. Mah, R.C.S. Wong, N.S.A. Manan, Y.L. Cheow, K.S. Sim, K. W. Tan, Group 6 photo-activable carbon monoxide-releasing molecules (PhotoCORMs) with 1′10-phenanthroline based ligand as potential anti-proliferative and anti-microbial agents, Inorg. Chim. Acta 537 (2022) 120931, https://doi.org/10.1016/j.ica.2022.120931.

[28] S.X. Lee, C.H. Tan, W.L. Mah, R.C.S. Wong, K.S. Sim, Y.L. Cheow, C.-H. Ng, K. W. Tan, Synthesis of phenanthroline-based ligand and its UV activable tetracarbonyl photoCORMs based on chromium, molybdenum, and tungsten as cytotoxic and antimicrobial agents, J. Organomet. Chem. 954-955 (2021) 122103, https://doi.org/10.1016/j.jorganchem.2021.122103.

[29] I.J.S. Fairlamb, J.M. Lynam, B.E. Moulton, I.E. Taylor, A.K. Duhme-Klair, P. Sawle, R. Motterlini, η^1-2-Pyrone metal carbonyl complexes as CO-releasing molecules (CO-RMs): a delicate balance between stability and CO liberation, Dalton Trans. (2007) 3603–3605, https://doi.org/10.1039/B707377A.

[30] H. Liu, P. Wang, Q. Zhao, Y. Chen, B. Liu, B. Zhang, Q. Zheng, Syntheses, toxicity and biodistribution of CO releasing molecules containing $M(CO)_5$ (M = Mo, W and Cr), Appl. Organomet. Chem. 28 (2014) 169–179, https://doi.org/10.1002/aoc.3105.

[31] T. Teles, A. Fernandes, M.J. Ferreira, L. Côrte-Real, F. Marques, J.D.G. Correia, L. G. Alves, Cyclam-based molybdenum carbonyl complexes as a novel class of cytotoxic agents, New J. Chem. 49 (2025) 5766–5772, https://doi.org/10.1039/D4NJ05233A.

[32] W.-Q. Zhang, A.J. Atkin, I.J.S. Fairlamb, A.C. Whitwood, J.M. Lynam, Synthesis and reactivity of molybdenum complexes containing functionalized alkynyl ligands: a photochemically activated CO-releasing molecule (PhotoCO-RM), Organometallics 30 (2011) 4643–4654, https://doi.org/10.1021/om200495h.

[33] C.C. Romão, W.A. Blättler, J.D. Seixas, G.J.L. Bernardes, Developing drug molecules for therapy with carbon monoxide, Chem. Soc. Rev. 41 (2012) 3571–3583, https://doi.org/10.1039/C2CS15317C.

[34] H.-I. Choi, A. Zeb, M.-S. Kim, I. Rana, N. Khan, O.S. Qureshi, C.-W. Lim, J.-S. Park, Z. Gao, H.-J. Maeng, J.-K. Kim, Controlled therapeutic delivery of CO from carbon monoxide-releasing molecules (CORMs), J. Control. Release 350 (2022) 652–667, https://doi.org/10.1016/j.jconrel.2022.08.055.

[35] A.M. Mansour, R.M. Khaled, G. Ferraro, O.R. Shehab, A. Merlino, Metal-based carbon monoxide releasing molecules with promising cytotoxic properties, Dalton Trans. 53 (2024) 9612–9656, https://doi.org/10.1039/D4DT00087K.

[36] R. Motterlini, L.E. Otterbein, The therapeutic potential of carbon monoxide, Nat. Rev. Drug Discov. 9 (2010) 728–743, https://doi.org/10.1038/nrd3228.

[37] D. Rocco, N. Busto, C. Pérez-Arnaiz, L. Biancalana, S. Zacchini, G. Pampaloni, B. Garcia, F. Marchetti, Antiproliferative and bactericidal activity of diiron and monoiron cyclopentadienyl carbonyl complexes comprising a vinyl-aminoalkylidene unit, Appl. Organomet. Chem. 34 (2020) e5923, https://doi.org/10.1002/aoc.5923.

[38] L. Biancalana, M. De Franco, G. Ciancaleoni, S. Zacchini, G. Pampaloni, V. Gandin, F. Marchetti, Easily available, amphiphilic diiron cyclopentadienyl complexes exhibit in vitro anticancer activity in 2D and 3D human cancer cells through redox

modulation triggered by CO release, Chem. Eur. J. 27 (2021) 10169–10185, https://doi.org/10.1002/chem.202101048.
[39] H. Chen, J.A. Parkinson, S. Parsons, R.A. Coxall, R.O. Gould, P.J. Sadler, Organometallic ruthenium(II) diamine anticancer complexes: Arene-nucleobase stacking and stereospecific hydrogen-bonding in guanine adducts, J. Am. Chem. Soc. 124 (2002) 3064–3082, https://doi.org/10.1021/ja017482e.
[40] H. Chen, J.A. Parkinson, R.E. Morris, P.J. Sadler, Highly selective binding of organometallic ruthenium ethylenediamine complexes to nucleic acids: novel recognition mechanisms, J. Am. Chem. Soc. 125 (2003) 173–186, https://doi.org/10.1021/ja027719m.
[41] J.R. Ascenso, C.G. de Azevedo, I.S. Gonçalves, E. Herdtweck, D.S. Moreno, M. Pessanha, C.C. Romão, Mixed-ring and indenyl analogues of molybdenocene and tungstenocene: preparation and characterization, Organometallics 14 (1995) 3901–3919, https://doi.org/10.1021/om00008a042.
[42] J.W. Faller, Chin-Chun Chen, M.J. Mattina, A. Jakubowski, Organometallic conformational equilibria. XVI. Steric effects on π-allyl and π-indenyl orientation in molybdenum and tungsten complexes, J. Organomet. Chem. 52 (1973) 361–386, https://doi.org/10.1016/S0022-328X(00)95158-1.
[43] J.R. Ascenso, I.S. Gonçalves, E. Herdweek, C.C. Romão, Ring slippage in indenyl derivates of molybdenum and tungsten, J. Organomet. Chem. 508 (1996) 169–181, https://doi.org/10.1016/0022-328X(95)05859-N.
[44] T. Kottke, D. Stalke, Crystal handling at low temperatures, J. Appl. Crystallogr. 26 (1993) 615–619, https://doi.org/10.1107/S0021889893002018.
[45] APEX2 Data Collection Software, Version 2012.4, Bruker AXS Inc., Delft, The Netherlands, 2012.
[46] SAINT+ Data Integration Engine, Version 8.37b, Bruker AXS Inc., Madison, WI, USA, 2015.
[47] G.M. Sheldrick, SADABS 2012/1, Bruker AXS Area Detector Scaling and Absorption Correction Program, Bruker AXS Inc., Madison, WI, USA, 2012.
[48] G.M. Sheldrick, A short history of SHELX, Acta Crystallogr. A Found. Adv. 64 (2008) 112–122, https://doi.org/10.1107/S0108767307043930.
[49] G.M. Sheldrick, SHELXT-2014, Program for Crystal Structure Solution, University of Göttingen, 2014.
[50] G.M. Sheldrick, SHELXL v. 2014/3, Program for Crystal Structure Refinement, University of Göttingen, 2014.
[51] E. Antonini, Interrelationship between structure and function in hemoglobin and myoglobin, Physiol. Rev. 45 (1965) 123–170, https://doi.org/10.1152/physrev.1965.45.1.123.
[52] A.J. Atkin, J.M. Lynam, B.E. Moulton, P. Sawle, R. Motterlini, N.M. Boyle, M. T. Pryce, I.J.S. Fairlamb, Modification of the deoxy-myoglobin/carbonmonoxy-myoglobin UV–Vis assay for reliable determination of CO-release rates from organometallic carbonyl complexes, Dalton Trans. 40 (2011) 5755–5761, https://doi.org/10.1039/C0DT01809K.
[53] H. Brunner, M. Muschiol, Optically active transition metal complexes, LV [1]. Preparation und stereochemistry of $[C_5H_5Mo(CO)_2NN']PF_6$ with NN' = ethylenediamine and propylenediamine, Z. Naturforsch. 33b (1978) 247–248, https://doi.org/10.1515/znb-1978-0230.
[54] S.A. Hauser, R.M. Reich, J. Mink, A. Pöthig, M. Cokoja, F.E. Kühn, Influence of structural and electronic properties of organomolybdenum(II) complexes of the type $[CpMo(CO)_3R]$ and $[CpMo(O_2)(O)R]$ (R = Cl, CH_3, CF_3) on the catalytic olefin epoxidation, Catal. Sci. Technol. 5 (2015) 2282–2289, https://doi.org/10.1039/C4CY01604A.
[55] J.W. Faller, R.H. Crabtree, A. Habib, Control of slippage and conformation in indenyl complexes, Organometallics 4 (1985) 929–935, https://doi.org/10.1021/om00124a022.
[56] F.-C. Liu, P.-S. Yang, C.-Y. Chen, G.-H. Lee, S.-M. Peng, Syntheses, structures, and dynamic properties of $M(CO)_2(\eta^3\text{-}C_3H_5)(L\text{–}L)(NCBH_3)$ (M = Mo, W; L–L = dppe, bipy, en), J. Organomet. Chem. 693 (2008) 537–545, https://doi.org/10.1016/j.jorganchem.2007.11.039.
[57] F.-C. Liu, T.-C. Tsai, Y.-L. Lin, C.-S. Lee, P.-S. Yang, J.-C. Wang, Syntheses, structures, and dynamic properties of $M(CO)_2(\eta^3\text{-}C_3H_5)(en)(X)$ (M = Mo, W; X = Br, N_3, CN) and $[(en)(\eta^3\text{-}C_3H_5)(CO)_2M(\mu\text{-}CN)M(CO)_2(\eta^3\text{-}C_3H_5)(en)]Br$ (M = Mo, W), J. Organomet. Chem. 695 (2010) 423–430, https://doi.org/10.1016/j.jorganchem.2009.10.031.
[58] T.E. Bitterwolf, J.T. Bays, B. Scallorn, C.A. Weiss, M.W. George, I.G. Virrels, J. C. Linehan, C.R. Yonker, Organic matrix and solution photochemical studies of (allyl)dicarbonyl(cyclopentadienyl)molybdenum compounds, Eur. J. Inorg. Chem. (2001) 2619–2624, https://doi.org/10.1002/1099-0682(200109)2001:10%3C2619::AID-EJIC2619%3E3.0.CO;2-7.
[59] M. Domínguez-García, C. Ortega-Zúñiga, E. Meléndez, New tungstenocenes containing 3-hydroxy-4-pyrone ligands: antiproliferative activity on HT-29 and MCF-7 cell lines and binding to human serum albumin studied by fluorescence spectroscopy and molecular modeling methods, J. Biol. Inorg. Chem. 18 (2013) 195–209, https://doi.org/10.1007/s00775-012-0964-2.
[60] N. Dunwoody, S.-S. Sun, A.J. Lees, Quantitative photochemistry and mechanisms for a series of rhodium dicarbonyl derivatives, Inorg. Chem. 39 (2000) 4442–4451, https://doi.org/10.1021/ic000395n.
[61] D.G. Carroll, S.P. McGlynn, Semiempirical molecular orbital calculations. V. The electronic structure of arenechromium tricarbonyls and chromium hexacarbonyl, Inorg. Chem. 7 (1968) 1285–1290, https://doi.org/10.1021/ic50065a004.
[62] P.E. Bloyce, R.H. Hooker, A.J. Rest, T.E. Bitterwolf, N.J. Fitzpatrick, J.E. Shade, Photochemistry of some manganese and chromium dinuclear metal carbonyl complexes in frozen gas matrices at *ca.* 12 K, J. Chem. Soc. Dalton Trans. (1990) 833–841, https://doi.org/10.1039/DT9900000833.
[63] D.M. Manuta, A.J. Lees, Emission and photochemistry of $M(CO)_4$(diimine) (M = Cr, Mo, W) complexes in room-temperature solution, Inorg. Chem. 25 (1986) 1354–1359, https://doi.org/10.1021/ic00229a012.
[64] X. Pan, C.E. Philbin, M.P. Castellani, D.R. Tyler, Photochemistry of organometallic halide complexes. Mechanisms for the formation of ionic products, Inorg. Chem. 27 (1988) 671–676, https://doi.org/10.1021/ic00277a020.
[65] W.R. Kitzmann, M.-S. Bertrams, P. Boden, A.C. Fischer, R. Klauer, J. Sutter, R. Naumann, C. Förster, G. Niedner-Schatteburg, N.H. Bings, J. Hunger, C. Kerzig, K. Heinze, Stable molybdenum(0) carbonyl complex for upconversion and photoredox catalysis, J. Am. Chem. Soc. 145 (2023) 16597–16609, https://doi.org/10.1021/jacs.3c03832.
[66] G. Morselli, C. Reber, O.S. Wenger, Molecular design principles for photoactive transition metal complexes: a guide for "photo-motivated" chemists, J. Am. Chem. Soc. 147 (2025) 11608–11624, https://doi.org/10.1021/jacs.5c02096.
[67] C.E. Borja, V. Jakúbek, A.J. Lees, Quantitative photochemistry of $(\eta^5\text{-}C_5H_5)Fe(CO)_2I$ in solution: effective heterolytic Fe-I dissociation upon long-wavelength excitation, Inorg. Chem. 37 (1998) 2281–2284, https://doi.org/10.1021/ic971231i.
[68] C.C.L. Pereira, P.J. Costa, M.J. Calhorda, C. Freire, S.S. Rodrigues, E. Herdtweck, C. C. Romão, Ring slippage vs charge transfer in the reductive chemistry of $[IndMo(CO)_2(\alpha\text{-diimine})]^+$ cations, Organometallics 25 (2006) 5223–5234, https://doi.org/10.1021/om050986r.
[69] H. Aritani, T. Tanaka, T. Funabiki, S. Yoshida, K. Eda, N. Sotani, M. Kudo, S. Hasegawa, Study of the local structure of molybdenum-magnesium binary oxides by means of Mo L_3-edge XANES and UV–Vis spectroscopy, J. Phys. Chem. 100 (1996) 19495–19501, https://doi.org/10.1021/jp9615464.
[70] R.P. Monteiro, I.B. Calhau, A.C. Gomes, A.D. Lopes, J.P. Da Silva, I.S. Gonçalves, M. Pillinger, β-Cyclodextrin and cucurbit[7]uril as protective encapsulation agents of the CO-releasing molecule $[CpMo(CO)_3Me]$, Dalton Trans. 54 (2025) 166–180, https://doi.org/10.1039/d4dt01863j.
[71] A. Kubicka, E. Parfieniuk, E. Fornal, M. Palusiak, D. Lizińska, A. Gumieniczek, B. Rudolf, Metallocarbonyl complexes: $(\eta^5\text{-}C_5H_5)M(CO)_n(\eta^1\text{-}N\text{-imidato})$ (M = Fe, Ru, Mo, W; n = 2, 3) as new photoactive CO-releasing molecules (CORMs), J. Photochem. Photobiol. A Chem. 351 (2018) 115–123, https://doi.org/10.1016/j.jphotochem.2017.10.012.
[72] M.A. Wright, J.A. Wright, PhotoCORMs: CO release moves into the visible, Dalton Trans. 45 (2016) 6801–6811, https://doi.org/10.1039/C5DT04849D.